

# Development of Concentrating Heliostats for High Temperature Solar Chemical Applications

Juan Pablo González-López<sup>1</sup>, Ricardo A Pérez-Enciso<sup>2</sup>, Carlos A Pérez-Rábago<sup>1</sup>, and Claudio A Estrada<sup>1,\*</sup>

<sup>1</sup> Instituto de Energías Renovables, Universidad Nacional Autónoma de México, Temixco, México.

<sup>2</sup> Universidad de Sonora, Hermosillo, Sonora.

\* Correspondence to C.A. Estrada, Privada Xochicalco S/N, Col. Centro, Temixco, Morelos, México. CP 62580.

**Abstract.** In the present paper, the design, construction, and evaluation of a concentrating spherical heliostat are shown; curved facets were achieved by a mechanical design. Furthermore, a comparison between a flat heliostat and the concentrating heliostat is performed. The evaluations were made at the facilities of the Solar Platform of Hermosillo, in the city of Hermosillo, Sonora, México.

**Keywords:** Heliostats, Concentrating Heliostats, Central Receiver Technology, CSP Technology

## 1. Introduction

Solar towers are often predicted to be one of the least expensive methods of producing solar-generated electricity and hydrogen on a large scale [1,2]. The history of heliostat design & development is well documented in several documents [3]. Other studies review the state of art of heliostat development [4]. Some heliostat plants have decided to focus their attention on concentrating heliostats [5]. In this project, the design and development of concentrating heliostats for solar thermochemical applications is focused. The Experimental Field of the Central Tower Technology (CEToC, for its acronym in Spanish) of the National Laboratory of Solar Concentration and Solar Chemistry (LACYQS – CONACYT, for its acronym in Spanish), which is located in the Solar Platform of Hermosillo, Mexico, has a solar tower 30 m high operating with 26 heliostats of 36 m<sup>2</sup> each. These heliostats produce a solar spot in the Lambertian target of approximately 6 m<sup>2</sup>. This solar tower system was initially thought as a proof and characterization field for heliostats manufactured for solar thermal power plants. This facility could be used for solar chemical applications if high concentrating rates are reached. The purpose of this paper is to explore the transformation of these heliostats into concentrating ones using the same structure (foundation, basic structure, mechanisms, etc.) to use this facility in studies of high-temperature solar chemistry applications [6]. Experimental Field of Central Tower Technology of the Solar Platform of Hermosillo (PSH, for its acronym in Spanish) is a facility that has been created jointly by the Universidad de Sonora and the Universidad Nacional Autónoma de México, mainly to carry out research, development and innovation about solar power tower technology. Conceived initially as the Experimental Field of Central Tower Technology (CEToC), these facilities also count with parabolic dish, lineal Fresnel and parabolic trough technology. Among the main services that the CEToC facilities offer are the design, proof and evaluation of components and subsystems as solar trackers, heliostats, solar receivers, thermal storage systems, and control systems. Broadly, the facilities are used as an essay and laboratory facility for

different applications that require high concentration rates of solar irradiation over relatively big surfaces. It is also performed research about thermodynamic cycles for electric generation from solar energy, solar chemistry, and photovoltaic systems with solar concentration. Figure 1 shows a picture of the CEToC with operating heliostats [5].



**Figure 1.** CEToC with heliostats in operation.

In Figure 2, on the left side, a layout of the position of the heliostats of the original CEToC design is shown. On the right side the positions of the current heliostats in operation are shown. Particularly, the positions of the F0 and F2 heliostats that will be studied in this work are pointed out.

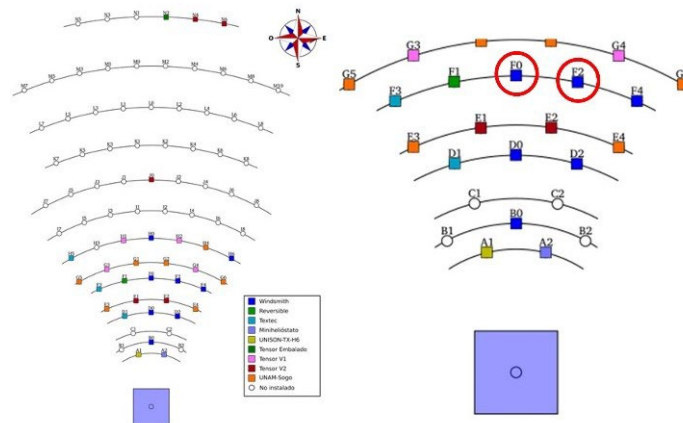


**Figure 2.** (Left) layout of the heliostats' position of the original CEToC. (Right) the positions of the current heliostats; heliostats circled in red are F0 and F2.

F0 and F2 heliostats are placed at a focal length of 72 m away from the Lambertian target. The rings schemed at Figure 2 represent different focal lengths away from the target. In this work, the focal length of 72 m was the focus of the project, as this is the hardest design to manufacture due to its slight curvature. Furthermore, focal lengths beyond this one implies that concentration is no more significant because of the half-angle subtended by the sun [6]. Figure 3 shows the three focal lengths involved in this project.

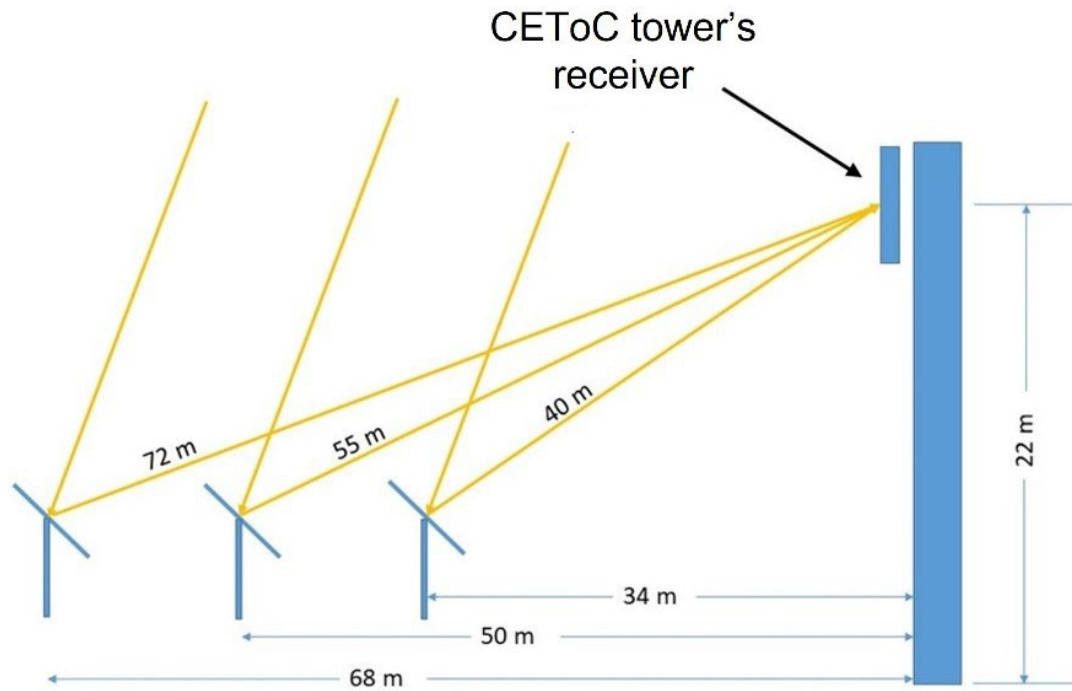


**Figure 3.** CEToC different focal lengths. F0 and F2 heliostats are placed at 72 m focal lengths.

## 2. Heliostats

### 2.1 Heliostat A: 36 m<sup>2</sup> heliostat with 25 flat and canted facets

The facility's current heliostats have 25 flat reflective facets. Figure 4 shows: a) the diagram of the structure of a heliostat and b) a photograph of the heliostat. The reflective surface consists of conventional 1.2 m x 1.2 m x 0.005 m mirrors. The mechanical structure of the facet consists of a 0.73 m x 0.73 m x 0.0381 m square tubular profile frame (current yellow frame in Figure 4). The mirror is fixed to the frame and then this frame is fixed to the heliostat's truss by means of ball joints, which allow the facets to be edged. The heliostat is made up of 25 of these flat facets in a 5x5 facet array (i.e., a square heliostat). This results in a reflective area of 36 m<sup>2</sup>. These heliostats deliver a 6 m<sup>2</sup> solar spot in the Lambertian target of the solar tower. Three different focal lengths are arranged in the field: 40 m, 55 m and 72 m.

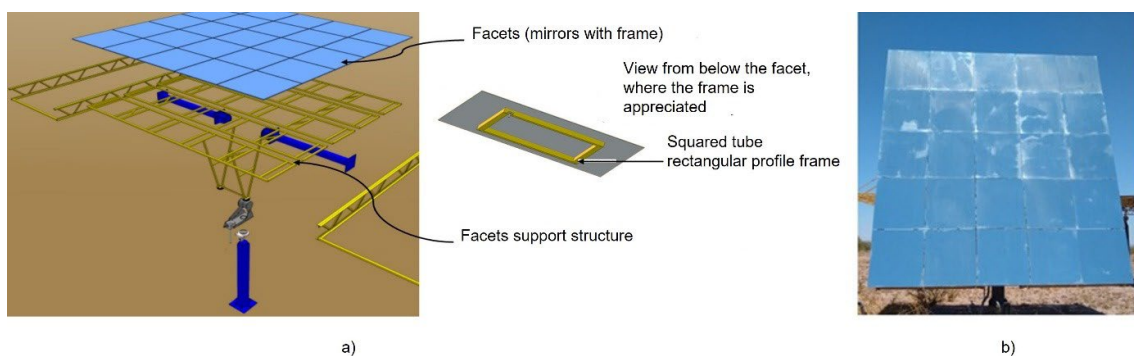


**Figure 4.** a) Exploded view of current heliostats with flat facets, and b) image of the flat heliostat F2 in operation.

## 2.2 Heliostat B: 36 m<sup>2</sup> heliostat with 25 spherical and canted facets

The new spherical facet consists of a 1.2 m x 1.2 m x 0.003 m conventional mirror. The width reduction of the mirror is to ensure a mechanical sag when bonding the mirror to the trellis. The mechanical structure includes the current frame, that is part of the flat facets. Above this frame, a cross-piece structure of tubular rectangular profile (0.0254 m x 0.0508 m) is fixed. This structure of crossbars supports a trellis at the top, which has a curved finish on the front edge. This curvature corresponds to the radius of curvature of 144 m. This trellis is made up of six 14-gauge metal sheets (1.20 m long and 0.10 m high). Three of them have a hole in the top edge and three have a hole in the bottom edge. These holes allow the metal sheets to fit into a square matrix. The Figure 5 shows the design and the composition of the spherical facet. Finally, the facets are fixed onto the heliostat's truss through the ball joints.

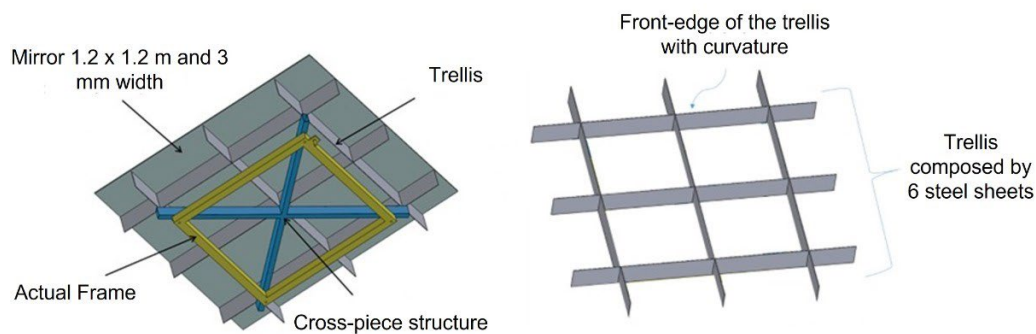


**Figure 5.** Structure of the new facet with spherical shape.

## 3. Optical study of the spherical facets

To test the hypothesis that spherical facets perform better than flat ones, a ray tracing simulation was performed. The software used for this ray-trace study is Tonatiuh, which is free access software made by CENER (National Center for Renewable Energies) and uses a MonteCarlo method to solve its simulations [7,8].

The experimental design was the placement of two mirrors: one with a flat surface and the other with a spherical surface, both of 1.2 x 1.2 m placed 72 meters from the objective on the tower. Both the flat and spherical facets were configured with an optical error of 1 mrad, a reflectivity of 1, and a DNI of 1000 W/m<sup>2</sup>.

The results are presented on Figure 6. In the left of Figure 6, the spot made by the flat facet is located at the left of the target, meanwhile the spherical facet spot is at the right. At the right of Figure 6 the profiles of both resulting spots are shown. Evidently, the spot produced by the spherical facet is three times more concentrated than the flat one, having a flux peak power of approximately 2250 W/m<sup>2</sup>, in comparison with the flat one of 750 W/m<sup>2</sup>.

Once the simulation was successful, a prototype of the spherical facet was fabricated and an experiment was carried out. The results of the experiment are given in Figure 7. A flat facet was compared with the spherical prototype. The normalized profiles produced by the planar facet and the spherical prototype are also shown. The facets were placed outside the optical axis of the tower-heliostat system to facilitate the experiment, which causes a slight elongation in the images, especially in the flat one.

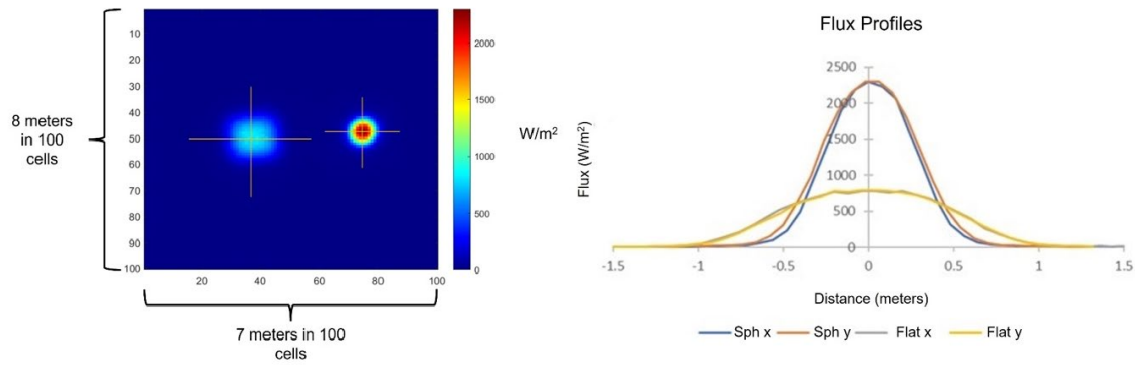


**Figure 6.** (Left) Resulting spots in the ray tracing simulation; on the left is the spot resulting from the flat facet and on the right the spot resulting from the spherical facet. (Right) Flow profiles resulting from the ray tracing simulation.

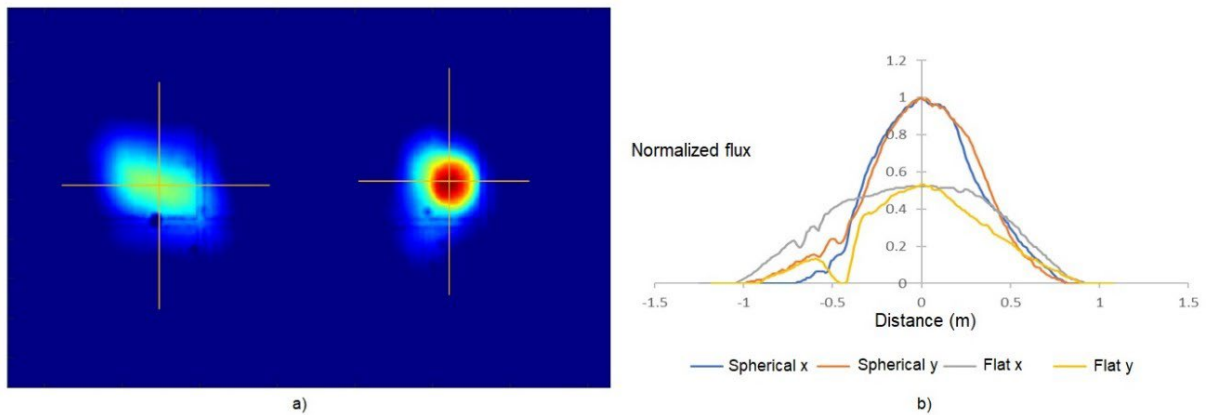


**Figure 7.** a) Spots produced by a flat (left) facet and a spherical prototype (right), and b) normalized flux profiles of the flat facet and the spherical prototype. Images were taken near the midday.

#### 4. Results of 25 manufactured spherical facets

25 spherical facets were manufactured and mounted on the truss of the heliostat. Neither the truss, foundation nor the tracking mechanisms were modified. The 25 facets deliver an area of  $36 \text{ m}^2$ , that corresponds to the area of the flat heliostat. The results varied between each facet, resulting in different spot areas and thus, in different rates of concentration. To know the upper theoretical limit of the concentration given by the 25 spherical facets individually, a manipulation of the given spots was performed. The peak fluxes of each spot were overlapped and thus, an ideal scenario of the spherical heliostat was obtained.

This is the best possible result when canting the concentrating heliostat. The result is shown in Figure 8. This Figure shows an ideal scenario, i.e., with a 0 mrad error due to the canting error (i.e., alignment). That is the upper empirical limit of the optical performance of this heliostat.

A canting campaign was performed during the first week of march, 2022. Canting was made in five days in a period of  $\pm 1$  hour from solar culmination. The results are presented on Figure 9, which presents the canted spherical heliostat. Concentration ratio peak in the theoretical upper limit (ideal spot) was of approximately 55 suns, whereas the concentration ratio peak in the canted heliostat was of approximately 35 suns. This suggests that the canting methodology must be improved to yield the upper limit. Nonetheless, the typical Gaussian

formis accomplished.

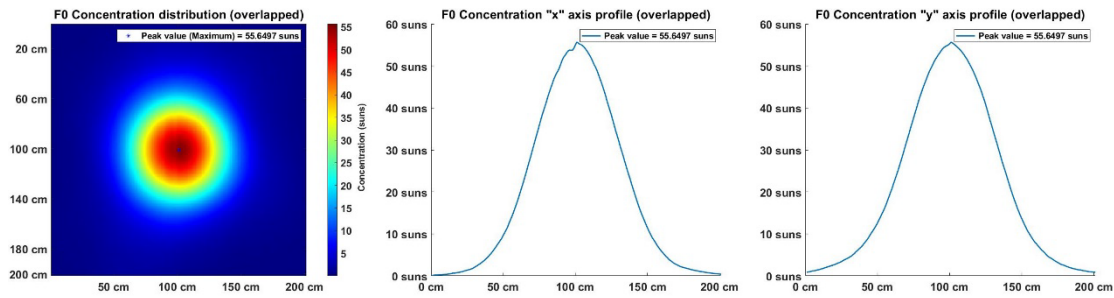


**Figure 8.** a) Resulting spot with all the superimposed images produced by the 25 facets. b) Flow profile on the "x" axis of the spot. c) Flow profile on the "y" axis of the spot.

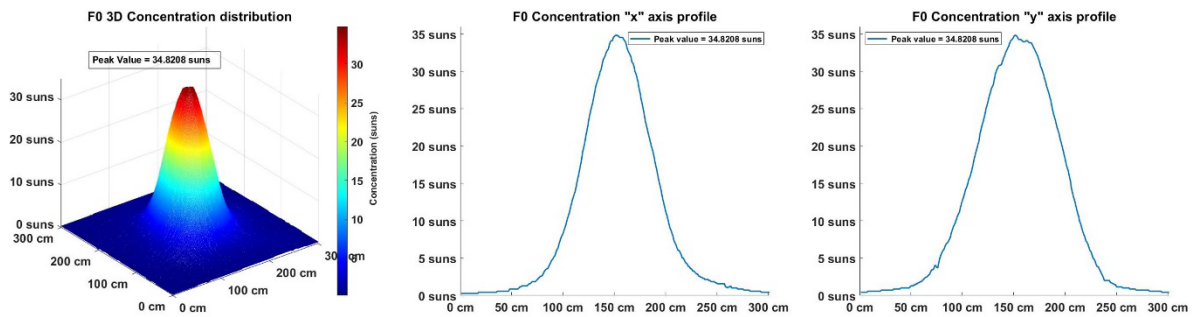


**Figure 9.** a) Concentration distribution of the canted spherical heliostat. b) "x" axis concentration profile. c) "y" axis concentration profile.

## 5. Comparison between the spherical heliostat and flat heliostat

A comparison of both heliostats was made. Figure 10 shows the comparative between the spherical heliostat and the flat heliostat. The images of the spherical heliostat were taken at solar noon at 16 of march, 2022, and the images taken of the flat heliostat were taken at solar noon at 22 of march, 2022. Images were taken using a CCD Pyke 8-bit camera.

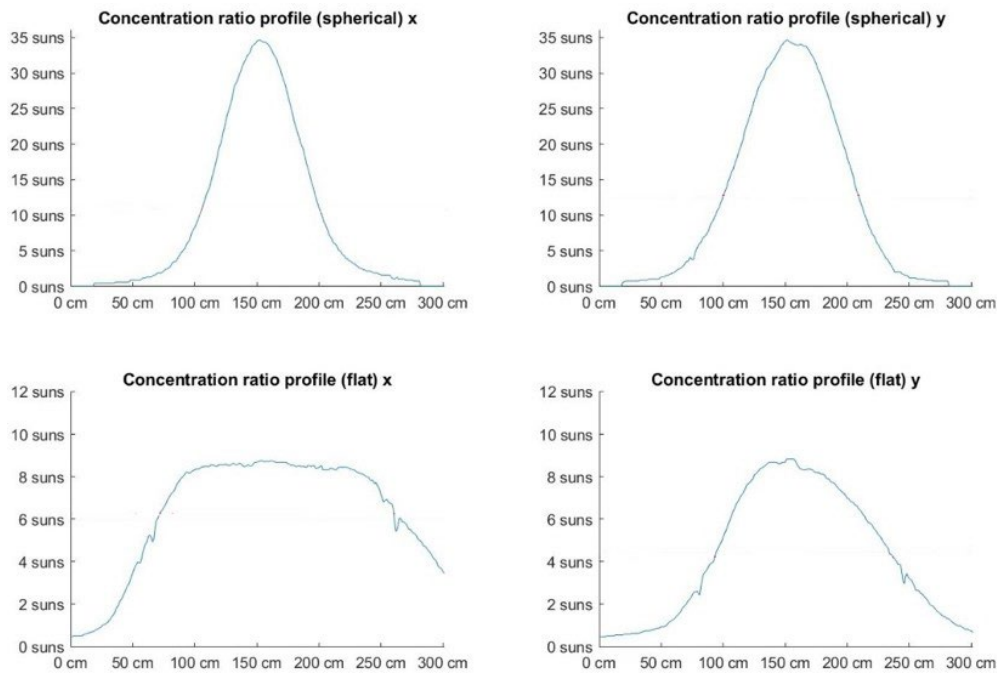


**Figure 10.** Solar concentration profiles in x and y slices for flat and spherical heliostats. All images taken at the corresponding solar noon.

This figure shows that the concentration ratio of the spherical heliostat exceeds that of the flat heliostat.

## 6. Conclusions

The design, construction and evaluation of spherical faceted heliostats were presented. A comparison was made between a flat facet and a spherical facet, finding that the spherical facet reaches concentration peaks twice that of the flat facet.

The images produced by the set of 25 spherical facets mounted on the structure of a heliostat were also compared, in comparison with the heliostats with flat facets. It was found that the concentration peaks of the heliostats with spherical facets reached 35 suns, while that of the flat facets was 8 suns.

The main conclusion is that spherical faceted heliostats increase the concentration ratio significantly.

## Data availability statement

Raw data were generated at Plataforma Solar de Hermsillo. Derived data supporting the findings of this study are available from the corresponding author C.A. Estrada on request.

## Author contributions

J.P. González-López: Methodology, Ray-tracing Analysis, Data Curation, Writing – Review and Editing, Visualization; R.A. Pérez-Enciso: Methodology, Ray-tracing Analysis, Technical Support, Supervision; C.A. Pérez-Rábago: Technical Support, Project Management; C.A. Estrada: Conceptualization, Methodology, Writing - Review and Editing, Visualization, Supervision, Resources.

## Competing interests

The authors declare no competing interests.

## Acknowledgements

The authors thank the University of Sonora and the National Autonomous University of Mexico for allowing us to use their facilities for experimentation. We also thank the DGAPA-UNAM for financing the project through the PAPIIT AG101422 grant. Likewise, Juan Pablo González thanks CONACYT for the scholarship he has.

## References

1. Achkari, O., & el Fadar, A. (2020). Latest developments on TES and CSP technologies –Energy and environmental issues, applications and research trends. In *Applied Thermal Engineering* (Vol. 167). Elsevier Ltd. <https://doi.org/10.1016/j.applthermaleng.2019.114806>.
2. Arbes, F., Weinrebe, G., Wöhrbach, M., 2016. Heliostat Field Cost Reduction By "Slope Drive " Optimization Azimuth-Elevation Tracking, Conference Proceedings SolarPACES 2015. Cape Town, South Africa.
3. Kolb, G., Lumia, R., Davenport, R., Thomas, R., Gorman, D., Jones, S., & Donnelly, M. (2007). Heliostat cost reduction study. <https://doi.org/10.2172/912923>.
4. Pfahl, A., Coventry, J., Röger, M., Wolfertstetter, F., Vásquez-Arango, J. F., Gross, F., Arjomandi, M., Schwarzbözl, P., Geiger, M., & Liedke, P. (2017). Progress in heliostat development. *Solar Energy*, 152, 3–37. <https://doi.org/10.1016/j.solener.2017.03.029>.
5. Romero, M., González-Aguilar, J., Sizmann, A., Batteiger, V., Falter, C., Steinfeld, A., Zoller, S., Brendelberger, S., & Lieftink, D. (2020). Solar-driven thermochemical production of sustainable liquid fuels from H<sub>2</sub>O and CO<sub>2</sub> in a heliostat field. *Proceedings of the ISES Solar World Congress 2019*, 1321–1332. <https://doi.org/10.18086/swc.2019.23.02>.
6. Laboratorio Nacional de Sistemas de Concentración Solar y Química Solar. (n.d.). Retrieved May 2, 2022, from <http://www.concentrationsolar.org.mx/>.
7. Rosales Valles, M. M. (2014). Diseño, puesta en operación y evaluación de un helióstato con facetas deformables [Universidad Nacional Autónoma de México]. [http://www.concentrationsolar.org.mx/images/pdf/tesis/m3\\_militza.pdf](http://www.concentrationsolar.org.mx/images/pdf/tesis/m3_militza.pdf)
8. Centro Nacional de Energías Renovables. (2017). Tonatiuh. (<https://www.cener.com/documentacion/TONATIUH.pdf>)